



Published in final edited form as:

Oncogene. 2017 March ; 36(11): 1546–1558. doi:10.1038/onc.2016.323.

Epithelial-Mesenchymal Transition of Ovarian Cancer Cells Is Sustained by Rac1 through Simultaneous Activation of MEK1/2 and Src Signaling Pathways

Dongdong Fang^{1,2}, Huijun Chen³, Jessica Y Zhu⁴, Wei Wang¹, Yong Teng^{5,6}, Han-Fei Ding⁶, Qing Jing⁷, Shi-Bing Su^{1,2}, and Shuang Huang^{1,2,4}

¹Research Center for Traditional Chinese Medicine Complexity System, Shanghai University of Traditional Chinese Medicine, Shanghai, China

²E-institute of Shanghai Municipal Education Committee, Shanghai University of Traditional Chinese Medicine, Shanghai, China

³Department of Obstetrics and Gynecology, Zhongnan Hospital of Wuhan University, Wuhan, Hubei Province, China

⁴Department of Anatomy and Cell Biology, University of Florida College of Medicine, Gainesville, FL, USA

⁵Department of Oral Biology, Dental College of Georgia, Augusta University, Augusta, GA, USA

⁶Georgia Cancer Center, Augusta University, Augusta, GA, USA

⁷Department of Cardiology, Changhai Hospital, Shanghai, China

Abstract

Epithelial-mesenchymal transition (EMT) is regarded as a crucial contributing factor to cancer progression. Diverse factors have been identified as potent EMT inducers in ovarian cancer. However, molecular mechanism sustaining EMT of ovarian cancer cells remains elusive. Here, we show that the presence of SOS1/EPS8/ABI1 complex is critical for sustained EMT traits of ovarian cancer cells. Consistent with the role of SOS1/EPS8/ABI1 complex as a Rac1-specific guanine nucleotide exchange factor, depleting Rac1 results in the loss of most of mesenchymal traits in mesenchymal-like ovarian cancer cells while expressing constitutively active Rac1 leads to EMT in epithelial-like ovarian cancer cells. With the aid of clinically tested inhibitors targeting various EMT-associated signaling pathways, we show that only combined treatment of MEK1/2 and Src inhibitors can abolish constitutively active Rac1-led EMT and mesenchymal traits displayed by mesenchymal-like ovarian cancer cells. Further experiments also reveal that EMT can be induced in epithelial-like ovarian cancer cells by co-expressing constitutively active MEK1

Users may view, print, copy, and download text and data-mine the content in such documents, for the purposes of academic research, subject always to the full Conditions of use: http://www.nature.com/authors/editorial_policies/license.html#terms

Address correspondence to: Shuang Huang, Department of Anatomy and Cell Biology, University of Florida College of Medicine, Gainesville, FL 32610. shuanghuang@ufl.edu or Shi-Bing Su, Research Center for Traditional Chinese Medicine Complexity System, Shanghai University of Traditional Chinese Medicine, Shanghai, China. shibingsu07@163.com.

CONFLICT OF INTEREST

The authors declare no conflict of interest.

and Src rather than either alone. As the activities of Erk and Src are higher in ovarian cancer cells with constitutively active Rac1, we conclude that Rac1 sustains ovarian cancer cell EMT through simultaneous activation of MEK1/2 and Src signaling pathways. Importantly, we demonstrate that combined use of MEK1/2 and Src inhibitors effectively suppresses development of intraperitoneal xenografts and prolongs the survival of ovarian cancer-bearing mice. This study suggests that cocktail of MEK1/2 and Src inhibitors represents an effective therapeutic strategy against ovarian cancer progression.

INTRODUCTION

Ovarian cancer is the gynecological cancer with the highest mortality rate and a 5-year survival rate has been almost unchanged in last 30 years, remaining at about 30%. High mortality rate of ovarian cancer is most likely to be caused by late diagnosis when patients are already in advanced stages (1). Standard treatment has been surgical debulking followed by chemotherapy (2). Although most patients respond initially, almost all of them will relapse and ultimately meet their demise due to metastasis (1). Therefore, finding ways to contain metastasis may represent effective therapeutic strategy to help ovarian cancer patient survival.

Epithelial-mesenchymal transition (EMT) is a phenomenon during which cells undergo transition from an epithelial to mesenchymal phenotype (3). Since cancer cells acquire the ability to invade and to migrate through the process of EMT, EMT is thus recognized as a prerequisite of metastasis (3–5). EMT can be induced by diverse factors that include transforming growth factor β (TGF β)/bone morphogenetic proteins (BMPs), receptor tyrosine kinases, Wnt and Notch signaling pathways (3–5). Recent studies have also established a strong connection between tumor microenvironment and EMT because hypoxia (6, 7), inflammation (8, 9) and oxidation stress (10), phenomenon commonly detected in tumor microenvironment, are potent EMT inducers. Signals triggered by these factors all converge on EMT-inducing transcriptional factors such as Snail, Slug, Twist, and Zeb1/2 that diminish the expression of epithelial-related genes such as E-cadherin and, at the same time, enhance the expression of mesenchymal-related genes such as vimentin (3–5).

Like other epithelial-derived tumors, extensive evidences have demonstrated EMT as a critical step for ovarian cancer progression (11, 12). Immunohistological analyses of both primary and metastatic ovarian carcinoma reveal that EMT is significantly associated with peritoneal metastasis and survival of ovarian cancer patients (13, 14). Correlation between EMT and aggressiveness of ovarian cancer is also supported by gene expression-based studies in which metastatic tumors generally exhibit mesenchymal signatures (15, 16). Moreover, overexpression of EMT-inducing transcription factors like Snail, Twist and Zeb1/2 is frequently associated with poor prognosis of ovarian cancer (16, 17). Importantly, factors provoking EMT in ovarian cancer cells generally promote ovarian cancer progression while factors suppressing EMT usually hinder cancer progression. For example, mucin 4 that induces EMT in ovarian cancer cells strongly fosters cancer progression and is often overexpressed in high grade ovary tumors (18). MicroRNA-200c that deters EMT, inhibits metastasis of CD117+CD44+ ovarian cancer stem cells (19). Another example that

highlights the importance of EMT in ovarian cancer progression is that chemo-resistant ovarian cancer cells frequently display significant mesenchymal traits (20). However, molecular mechanism sustaining mesenchymal phenotype of ovarian cancer cells is poorly understood.

We previously discovered that SOS1/EPS8/ABI1 complex is critically associated with ovarian cancer aggressiveness (21). In this study, we show that sustained EMT necessitates the presence of SOS1/EPS8/ABI1 complex because depleting any component of this complex resulted in the loss of EMT traits in mesenchymal-like ovarian cancer cells while restoring an intact SOS1/EPS8/ABI1 complex in epithelial-like ovarian cancer cells confer them with mesenchymal characteristics. Consistent with the role of SOS1/EPS8/ABI1 complex as a Rac1-specific guanine nucleotide exchange factor (GEF), knockdown of Rac1 repressed EMT in mesenchymal-like ovarian cancer cells while expressing constitutively active Rac1 led to the occurrence of EMT in epithelial-like ovarian cancer cells. With the aid of clinically tested small molecule inhibitors targeting distinct EMT-associated signaling pathways, we show that combined use of MEK1/2 (AZD6244) and Src inhibitors (AZD0530), but not either alone, abolished Rac1-led EMT and also suppressed mesenchymal traits. These results raise the possibility that simultaneous activation of MEK1/2 and Src is required for sustained EMT in ovarian cancer cells. This possibility is supported by the observation that forced expression of both constitutively active MEK1 and Src, rather than either alone, led to EMT in epithelial-like ovarian cancer cells. Our data also indicate that Rac1-MEK/Src signaling pathway most likely promotes EMT by upregulating the expression of Twist and Zeb1/2. Finally, we demonstrate that cocktail of AZD6244 and AZD0530 effectively suppressed intraperitoneal xenograft development and prolonged the survival of ovary tumor-bearing mice.

RESULTS

Presence of SOS1/EPS8/ABI1 complex is essential for sustained EMT in ovarian cancer cells

We previously screened a panel of established ovarian cancer cell lines for their capability to develop intraperitoneal xenograft and identified ES2, HEY, OCC1, OVCAR5 and SK-OV3 as capable lines whereas HEC1A, IGROV1, OVCAR3 and TOV21G as incapable ones (21, 22). Given the close correlation between the capability to develop intraperitoneal xenograft and the potential of peritoneal metastasis among ovarian cancer cells (22), we examined EMT traits of these lines by determining their E-cadherin/vimentin expression and *in vitro* invasiveness. Western blot showed that lines with the capability to develop intraperitoneal xenografts all displayed robust level of vimentin (a mesenchymal marker) (Fig. 1A) and were able to invade Matrigel gel (Fig. 1B). With the exception of IGROV1, lines incapable of developing intraperitoneal xenograft expressed E-cadherin (an epithelial marker) and exhibited no detectable vimentin (Fig. 1A). Moreover, these lines were unable to invade Matrigel gel (Fig. 1B). These results demonstrate that lines with capability for intraperitoneal xenograft development exhibit EMT characteristics.

As we previously revealed that the presence of SOS1/EPS8/ABI1 complex is critical for the development of intraperitoneal xenograft in ovarian cancer cells (21), We next investigated a

potential functional link between EMT and SOS1/EP8/ABI1 complex by lentivirally silencing SOS1, EP8 or ABI1 in OVCAR5 and SK-OV3 cells. Western blotting showed that knockdown of any of them reduced the level of vimentin while induced E-cadherin expression (Fig. 1C). Matrigel invasion assay further showed that depleting any of them impaired the capability of OVCAR5 and SK-OV3 cells to invade Matrigel (Fig. 1D). In parallel experiments, we introduced ABI1 into ABI1-negative OVCAR3, EP8 into EP8-negative IGROV1 and SOS1 into SOS1-negative TOV21G cells. Their forced expression resulted in the induction of vimentin and disappearance of E-cadherin in these cells (Fig. 1E). Moreover, these cells became highly invasive (Fig. 1F). These results suggest that SOS1/EP8/ABI1 complex is critically linked to the sustained EMT characteristics of ovarian cancer cells.

Rac1 regulates EMT in ovarian cancer cells

SOS1/EP8/ABI1 complex is a Rac1-specific GEF that mediates Ras-induced Rac1 activation (23). The observation that sustained EMT is regulated by SOS1/EP8/ABI1 complex (Fig. 1) raises the possibility that Rac1 is involved in ovarian cancer cell EMT. To test this possibility, we augmented Rac1 activity in epithelial-like OVCAR3 and HEC1A cells by forcing the expression of constitutively active Rac1 (Myc-Rac1G12V) (Fig. 2A and S1A). Both Western blotting and immunofluorescence staining showed that expression of Rac1G12V diminished E-cadherin while induced vimentin expression in both cell lines (Fig. 2A and 2B). Upon microscopic observation, OVCAR3 and HEC1A cells with Rac1G12V expression displayed an elongated mesenchymal morphology, whereas control cells exhibited a cobble stone-like epithelial phenotype (Fig. 2C). Analysis of cell shapes with the aid of Image J software revealed that the ratio of length to width in cells with Rac1G12V expression was at least twice of that in control cells (Fig. 2D). Moreover, forced expression of Rac1G12V rendered both OVCAR3 and HEC-1A lines capable of invading Matrigel (Fig. 2E).

We next lentivirally introduced Rac1 shRNAs into mesenchymal-like OVCAR5 and SK-OV3 cells. Knockdown of Rac1 reduced more than 60% of endogenous Rac1 activity judging by the amount of GTP-bound Rac1 (Fig. S1B). Western blotting and immunofluorescence staining showed that silencing Rac1 led to the induction of E-cadherin and reduction of vimentin in these cells (Fig. 3A and 3B). Moreover, Rac1-knockdown cells exhibited an epithelial morphology while control cells displayed a mesenchymal phenotype (Fig. 3C). Analysis of cell shapes revealed that ratio of length to width in Rac1-knockdown cells was reduced more than 50% compared with control cells (Fig. 3D). Matrigel invasion assay further showed that these cells displayed greatly reduced *in vitro* invasiveness (Fig. 3E). These results suggest that Rac1 plays a critical role in EMT of ovarian cancer cells.

Activation of both MEK1/2 and Src signaling pathways is required for Rac1-led ovarian cancer cell EMT

EMT can be induced by multiple signaling pathways including TGF β , Notch, Wnt/ β -catenin, NF- κ B and receptor tyrosine kinases (RTKs) either alone or in cooperation (8, 24–28). Rac1 has also been previously reported to regulate EMT in breast cancer cells through the regulation of p21-activated kinase (PAK) and reactive oxygen species (ROS) (29, 30). To

determine downstream signaling pathways mediating Rac1-led EMT in ovarian cancer cells, we treated OVCAR3/Rac1G12V cells with inhibitors specific for various signaling molecules: AZD6244 for MEK1/2, LY2109761 for T β RI/II kinase inhibitor, FH535 for Wnt, TPCA1 for IKK2, LY450139 for γ -secretase (Notch), FRAX597 for PAK, Genistein for tyrosine kinase, AZD0530 for Src, N-acetyl-cysteine for ROS, Wortmannin for PI3K, TAK-715 for p38 and SP600125 for JNK (Supplemental Table 1). Among these inhibitors, AZD6244 and AZD0530 were able to partially restore E-cadherin in OVCAR3/Rac1G12V cells though they did not significantly alter the level of vimentin (Fig. 4A). Interestingly, combined treatment of AZD6244 and AZD0530 greatly enhanced the amount of both E-cadherin mRNA and protein whereas also diminished vimentin mRNA and protein in both OVCAR3/Rac1G12V and HEC1A/Rac1G12V cells (Fig. 4B and 4C). Microscopic analysis further showed that mesenchymal morphology of OVCAR3/Rac1G12V and HEC1A/Rac1G12V cells was reverted back to epithelial one (Fig. 4D).

In subsequent experiments, we analyzed the effect of AZD6244 and AZD0530 on EMT traits of OVCAR5 and SK-OV3 cells. QRT-PCR showed that both inhibitors in individuality were able to moderately induce E-cadherin mRNA while displayed only marginal effect on vimentin mRNA (Fig. 5A). In contrast, treating these cells simultaneously with both inhibitors led to much greater induction of E-cadherin mRNA and significant reduction in vimentin mRNA (Fig. 5A). Similarly, western blotting showed that combined use of AZD6244 and AZD0530 led to dramatic increase in the abundance of E-cadherin and disappearance of vimentin in both lines (Fig. 5B). In addition, mesenchymal morphology of OVCAR5 and SK-OV3 cells was largely changed to epithelial-like one upon the combined treatment of AZD6244 and AZD0530 (Fig. 5C). Moreover, combined treatment of AZD6244 and AZD0530 greatly slowed the rate of both lines to fill the gap in wound-healing assay (Fig. 5D) and also inhibited cell migration measured by Transwell assay (Fig. 5E and 5F). Taken together, these results suggest that Rac1-led EMT requires the activation of both MEK1/2 and Src signaling pathways.

Simultaneous activation of MEK1 and Src is sufficient to induce EMT—To further link MEK1/2 and Src signaling pathways to Rac1-led EMT, we analyzed the activation status of MEK1/2 and Src signaling pathways through the detection of extent of Erk and Src phosphorylation. Western blotting revealed that levels of phosphorylated Erk and Src were much higher in Rac1G12V-expressing OVCAR3 and HEC1A cells than their respective control cells (Fig. 6A). In a parallel experiment, we also observed that knockdown of Rac1 led to dramatic reduction in the levels of phosphorylated Erk and Src in SK-OV3 and OVCAR5 cells compared to control (Fig. 6B). These results indicate that Rac1 activation leads to higher activities of MEK1/2 and Src signaling pathways. Since activation of MEK/Erk can be downstream of Src and vice versa, we tested the effect of AZD0530 (blocking Src) on phosphor-Erk and AZD6244 (blocking MEK1/2) on phosphor-Src in OVCAR3/Rac1G12V cells. Western blotting showed that AZD0530 blocked Src phosphorylation but did not alter the level of phosphor-Erk (Fig. S2). Similarly, AZD6244 diminished Erk phosphorylation while displayed no effect on the abundance of phosphorylated Src (Fig. S2). These results not only confirm the specificities of these

inhibitors but also indicate that Rac1 activates MEK1/2 and Src signaling pathways in parallel rather sequentially.

We next introduced constitutively active MEK1 (MEK1-DD) and Src (Src-Y527F) into OVCAR3 or HEC1A cells individually or together. Forced expression of either MEK1-DD or Src-Y527F mutant slightly decreased E-cadherin while moderately increased amount of vimentin in both lines (Fig. 6C and 6D). However, simultaneously expressing both MEK1-DD and Src-Y527F mutants markedly diminished E-cadherin while caused a robust vimentin expression (Fig. 6C and 6D). These results are clearly consistent with the notion that concerted action of MEK1/2 and Src signaling pathways downstream of Rac1 facilitates EMT in ovarian cancer cells. Moreover, we observed that OVCAR3 and HEC1A cells co-expressing MEK1-DD and Src-Y527F were highly migratory while their respective control cells were little migratory as measured by Transwell assay (Fig. 6E). Microscopic observation also indicated the occurrence of EMT in OVCAR3 and HEC1A cells co-expressing MEK1-DD and Src-Y527F as they exhibited typical mesenchymal morphology (Fig. 6F).

Activities of MEK1/2 and Src are critical for upregulation of Twist and Zeb1/2 in ovarian cancer cells—To further elucidate molecular mechanism underlying Rac1-led EMT, we performed an expression array to assess the change in the levels of 84 EMT-associated genes using total RNA isolated from control and Rac1G12V-expressing OVCAR3 cells. Compared with the control, 29 genes increased, 22 decreased and 35 unchanged in OVCAR3/Rac1G12V cells (Supplemental Table 2). Level of E-cadherin (CDH1) was found to be decreased by 64-fold while vimentin (Vim) increased over 32-fold in OVCAR3/Rac1G12V cells when compared with the control (Supplemental Table 2), consistent with the change in their protein abundance detected by Western blotting (Fig. 2A). Further assessment of genes in which their expression was altered also revealed that the levels of Twist, Zeb1 and Zeb2, three key EMT-inducing transcription factors were much higher in OVCAR3 or HEC1A cells expressing Rac1G12V when compared with the control (Supplemental Table 2, Fig. 7A and S3A). Subsequent analysis also showed that amount of Twist, Zeb1 and Zeb2 mRNA was increased by the expression of MEK1-DD or Src-527D, and in much greater extent by them together (Fig. 7B and S3B). In addition, analysis of established ovarian cancer cell lines revealed that Twist, Zeb1 and Zeb2 mRNA were generally higher in metastatic (mesenchymal-like) ovarian cancer cell lines than non-metastatic (epithelial-like) ones (Fig. 7C).

To investigate the importance of MEK1/2 and Src signaling pathways in Twist and Zeb1/2 expression, we treated OVCAR3/Rac1G12V and SK-OV3 cells with AZD6244 and AZD0530 either alone or together. QRT-PCR showed that levels of Twist, Zeb1 and Zeb2 mRNA were moderately decreased by MEK1/2 inhibitor AZD6244 but little altered by Src inhibitor AZD0530 (Fig. 7D). In contrast, combined treatment of AZD6244 and AZD0530 greatly downregulated the expression of all three transcription factors (Fig. 7D). Taken together, these results implicate that upregulation of Twist and Zeb1/2 is at least one of the contributing factors for Rac1-MEK/Src signaling axis-led EMT in ovarian cancer cells.

Combined use of MEK and Src inhibitors inhibits intraperitoneal xenograft development and prolongs the survival of ovary tumor-bearing mice

The observation that the combined use of AZD6244 and AZD0530 blocked EMT in ovarian cancer cells prompted us to investigate the efficacy of these two inhibitors to suppress ovarian cancer cell invasion. Matrigel invasion assay showed that either inhibitor alone was able to inhibit the ability of OVCAR3/RacG12V and SK-OV3 cells to invade Matrigel and combined use almost completely abrogated invasion (Fig. S4). To determine their effect on ovary tumor development, female athymic nude mice were intraperitoneally injected with luciferase-expressing OVCAR3/Rac1G12V or SK-OV3 cells for 12 days followed by orally administering AZD6244 and AZD0530 either alone or together to animals (Fig. 8A). Bioluminescence imaging showed that intraperitoneal xenografts could be detected 12 days after tumor cell injection (Fig. 8B). Tumors propagated rapidly in mice injected with OVCAR3/Rac1G12V cells (Fig. 8B) and mice died between 4 to 5 weeks (Fig. 8C). Efficient intraperitoneal xenograft development was also observed in mice receiving SK-OV3 cells (Fig. 8B). The earliest morbidity of mice receiving SK-OV3 cells occurred between 2–3 weeks and all mice died within 8 weeks (Fig. 8C). Administering AZD0530 alone to mice injected with OVCAR3/Rac1G12V cells did not significantly inhibit tumor propagation or prolong the survival ($p = 0.78$) while it was moderately effective in decreasing tumor burden and prolonging survival of mice receiving SK-OV3 cells ($p < 0.05$) (Fig. 8B and 8C). In contrast, administering AZD6244 alone significantly deterred tumor propagation and increased the lifespan of mice receiving either OVCAR3/Rac1G12V or SK-OV3 cells ($p < 0.01$) (Fig. 8B and 8C). When AZD0530 and AZD6244 were simultaneously given to animals, tumor progression was suppressed much more effectively than using either inhibitor alone ($p < 0.001$) (Fig. 8B). Animals receiving both AZD0530 and AZD6244 also survived significantly longer ($p < 0.001$) (Fig. 8C). To link deterred intraperitoneal xenograft development to blocked MEK/Src signaling and EMT, we performed immunohistochemistry to examine the intensity of phosphorylated Erk1/2, phosphorylated Src, E-cadherin and vimentin staining on collected tumors. Strong phosphor-Src, phosphor-Erk and vimentin but no E-cadherin staining were detected in tumors derived from OVCAR3/Rac1G12V and SK-OV3 cells (Fig. 8D). Tumors derived from mice administered with AZD0530 or AZD6244 were negative for phosphor-Src and phosphor-Erk staining respectively (Fig. 8D), confirming their ability to target intended pathways. Compared with control, tumors derived from AZD0530 or AZD6244 treatment group also displayed much less vimentin staining (Fig. 8D). Interestingly, E-cadherin staining was only observed in mice treated with both AZD0530 and AZD6244 (Fig. 8D). These results suggest that upregulation of vimentin and downregulation of E-cadherin in ovary tumors depend on simultaneous activation of both MEK1/2 and Src signaling pathways, thus supporting the notion that deterred tumor progression and prolonged survival of tumor-bearing mice by AZD0530 and AZD6244 are likely to be the consequence of their suppressive effect on EMT.

DISCUSSION

Role of EMT in ovarian cancer malignancies is supported by the findings that mesenchymal-like gene expression signature is generally associated with aggressive and metastatic ovarian cancer (13, 14). It is also backed by the findings that factors inducing EMT often act as

metastasis promoters (11). Here, we observed that ovarian cancer cell lines capable of developing intraperitoneal xenografts are mesenchymal in nature while lines incapable of developing intraperitoneal xenografts exhibited epithelial-like phenotype (Fig. 1). We previously discovered that the presence of SOS1/EP8/ABI1 complex is critical for development of intraperitoneal xenografts of ovarian cancer cells (21). In this study, we detected that ovarian cancer cell lines with an intact SOS1/EP8/ABI1 complex all displayed EMT traits, and disrupting SOS1/EP8/ABI1 complex by depleting members of this complex led to the suppression of EMT in mesenchymal-like ovarian cancer cells while restoring an intact SOS1/EP8/ABI1 complex converted epithelial-like ovarian cancer cells to mesenchymal-like ones (Fig. 1). Given a close correlation between capability of intraperitoneal xenograft development and metastatic potential in ovarian cancer cells, our data suggest that SOS1/EP8/ABI1 complex may control ovarian cancer metastasis by sustaining EMT in ovarian cancer cells.

SOS1/EP8/ABI1 complex is a GEF specifically activating Rac1 (23). The importance of SOS1/EP8/ABI1 complex in ovarian cancer cell EMT indicates that this complex may regulate EMT through Rac1. Rac1 has been shown to participate in EMT of diverse cancer cell types. For example, Rac1 mediates EMT induced by IRGM1 in melanoma cells (31), interferon regulatory factor 4 binding protein in breast cancer cells (32) and Twist in head and neck squamous carcinoma cells (33). In this study, we showed that silencing Rac1 diminished EMT characteristics of mesenchymal-like ovarian cancer cells while ectopically expressing constitutively active Rac1 resulted in EMT in epithelial-like ovarian cancer cells (Fig. 2 and 3). These findings strongly implicate Rac1 as an EMT executor in ovarian cancer cells. A recent study reported that Rac1 overexpression was closely associated with advanced stage of ovarian cancer and poor prognosis (34). We previously found that blocking Rac1 activity with dominant negative Rac1 suppressed peritoneal metastatic colonization (21). These observations are evidently in agreement with the notion that Rac1 impacts ovarian cancer progression and metastasis by promoting EMT. Several recent studies indicate the potential role of RhoA/RhoC in ovarian cancer EMT. For instance, BMP4, which induces EMT in ovarian cancer cells, also activates RhoA (35). Soft matrices increased ovarian cancer malignancy by facilitating EMT in a RhoA-dependent mechanism (36). Moreover, ectopic RhoC expression was shown to induce EMT in ovarian cancer cells and its presence appears to be important for growth factor-induced EMT (37). It will be of great interest to investigate whether Rho facilitates ovarian cancer EMT in a similar mechanism as we identified for Rac.

Diverse signaling pathways have been linked to EMT in various cancer cell types (3–5). With the aid of specific inhibitors, we found that deterrence of EMT requires simultaneous inhibition of both MEK1/2 and Src signaling pathways in constitutively active Rac1-expressing epithelial-like or established mesenchymal-like ovarian cancer cells (Fig. 4, 5 and 7). We further showed that expressing constitutively active MEK1 and Src together, rather than either alone led to the occurrence of EMT in epithelial-like ovarian cancer cells (Fig. 6, 7 and S3). A recent study showed that Src inhibitor (AZD0530) was able to restore E-cadherin expression in at least some ovarian cancer cell lines (38). Another study reported that tissue transglutaminase induced ovarian cancer cell EMT in a Src-dependent mechanism (39). Moreover, CrkL was reported to regulate CCL19/CCR7-induced ovarian cancer cell

EMT via MEK1/2 signaling pathway (40). Although results from these studies pinpoint the importance of MEK1/2 and Src signaling pathway in ovarian cancer EMT, we are the first to demonstrate that a complete ovarian cancer cell EMT is actually sustained by the simultaneous activation of both MEK1/2 and Src signaling pathways downstream of Rac1.

Through the analyses of clinical specimens, activation of MEK1/2 and Src signaling pathways has been found to be associated with EMT features and disease progression of various cancer types. For instance, EMT features (increased vimentin/fibronectin and decreased E-cadherin) were found to be associated with the elevated level of activated Erk in surgical resected pancreatic tumor specimens and are the prognostic indicator for poor survival (41). In clinical head and neck squamous carcinoma specimens, level of activated Src was shown to negatively correlate with E-cadherin expression but positively associate with the abundance of vimentin and aggressive tumor characteristics (42). Although the association between EMT and activation status of MEK1/2 and Erk signaling pathways has not been investigated in clinical ovarian tumor specimens, our results generated from multiple established ovarian cancer cell lines and these previous findings with other cancer types strongly support the existence of such correlation in ovary tumors.

The well recognized importance of EMT in cancer progression implicate that interfering with Rac1 activity may represent an effective strategy to suppress ovary tumorigenesis. This possibility is supported by earlier finding that dominant negative Rac1 completely abolished intraperitoneal xenograft development of ovarian cancer cells (21). Unfortunately, strategy of directly targeting Rac1 is currently unavailable because efforts on developing clinically applicable Rac1 inhibitor have not been successful (43). Our current study shows that Rac1 promotes EMT through simultaneous activation of MEK1/2 and Src signaling pathways. We thus reason that we may achieve the goal of interfering with Rac1 function by simultaneously targeting MEK1/2 and Src. Such strategy is apparently very feasible because of the availability of MEK1/2 and Src inhibitors that are already in phase II clinical trials. Our reasoning is evidently supported by our observation that combined use of MEK1/2 (AZD6244) and Src inhibitors (AZD0530) suppressed metastatic colonization of ovarian cancer cells and prolonged the survival of mice bearing ovary tumors (Fig. 8). In conclusion, our study has laid a foundation on using currently available MEK1/2 and Src inhibitors to treat advanced ovary tumors.

MATERIALS AND METHODS

Cells, shRNAs, and other reagents

All cells were maintained in DMEM containing 10% FBS at 37°C in a humidified incubator supplied with 5% CO₂. The shRNA sequences for Rac1 were designed using web-based Block-iT program (Life Technologies, Carlsbad, CA) and subcloned into pLV-shRNA vector (Biosettia, San Diego, CA). Expression and shRNA constructs for EPS8, ABI1 and SOS1 were described previously (21). Expression vectors for MEK1-DD and Src-Y527F were purchased from Addgene (Cambridge, MA) and the coding sequences for MEK1-DD and Src-Y527F were subcloned into lentiviral expression vector pCDH (System Biosciences, Mountain View, CA). All inhibitors were purchased from commercial sources and described

in Supplemental Table 1. Information for Rac1 shRNA sequences, primer sequences for PCR and antibodies are included in Supplementary Information.

Western blot analysis

Cells in monolayer were washed with phosphate-buffered saline (PBS) and harvested with radio-immunoprecipitation assay lysis (RIPA) buffer. Cell lysates were electrophoresed on 10–12% SDS-polyacrylamide gels, then transferred onto nitrocellulose membranes and membranes were incubated overnight at 4°C with primary antibodies. After several washes, membrane were incubated with HRP-conjugated secondary antibodies for 1 h at room temperature and developed with SuperSignal West Femto Kit (ThermoFisher Scientific, Waltham, MA).

Immunofluorescence staining and cell shape analysis

Cells seeded on coverslips were washed with ice-cold PBS and then blocked with 5% heat-denatured bovine serum albumin. After membrane permeabilization with 0.5% Triton-X100, cells were stained using anti-E-cadherin monoclonal antibody or anti-vimentin polyclonal antibody followed by fluorescein or rhodamine-conjugated secondary antibodies for another hour. Nuclei were visualized by staining with 4',6-diamidino-2-phenylindole (DAPI). The fluorescence staining was observed with the aid of a fluorescence microscope (Axiovert 200M; Carl Zeiss, Thornwood, NY). To analyzed cell shape, both length and width cell size (length:width ratio) was measured using Image J software in > 100 cells. Cell length was defined by the longest distance between any two points of the cell, and cell width was measured as the longest line perpendicular to the cell-length line.

In vitro invasion and cell migration assay

In vitro invasion assay was performed using Matrigel invasion chambers (Cell Biolabs, San Diego, CA) as previously described (21, 44, 45). Briefly, 2×10^5 cells were plated into each of invasion chamber and medium containing 10% fetal calf serum was added into lower chamber. Cells were allowed to invade for 24 h followed by removing remaining cells in the invasion chambers by cotton swab. Cells on the undersurface of invasion chambers were stained with crystal violet and counted under a phase-contrast microscope. Cell migration was measured with the aid of Transwells (8.0mm pore size) as described previously (46–48). Briefly, the undersurface of Transwell was coated with 10µg/mL of collagen I and serum-free medium was added to lower chambers. Serum-starved cells (10^5 cells in 100µl/well) were first treated with 5µM AZD6244 and 0.5µM AZD0530 either alone or together for 24 h, then added to Transwells and allowed to migrate for 24 h. Cells remained in Transwells were removed with cotton swabs, and cells attached on undersurface were stained with crystal violet solution for visualization. To quantitate cell migration, stained cells on the undersurface were solubilized with 10% acetic acid and measured at 600 nm on a BioRad microplate reader.

Rac1 activity assay

Rac activity assay was determined using G-LISA Rac1 Activation assay Kit (Cytoskeleton, Denver, CO) according to the manufacturer's instructions. Briefly, overnight-cultured cells

were lysed and cell lysates were used to measure Rac1 activity on an ELISA-formatted and colorimetric-based assay.

Real time PCR-based microarray assay and qRT-PCR

Effect of constitutively active Rac1 on the expression of genes associated with EMT was analyzed using human EMT RT2 Profiler PCR Array (Qiagen, Frederick, MD). Total RNA isolated from control OVCAR3 and OVCAR3/Rac1V12 cells was used for screening as per the manufacturer's instructions. Some of the genes in which their expression were differentially regulated at least 2 fold difference were further validated by qRT-PCR using total RNA isolated from a panel of ovarian cancer cell lines. For qRT-PCR, total RNA was treated by DNase I and then reverse transcribed with SuperScriptase II (Life Technologies). Generated cDNA was subjected to quantitative PCR with specific primer sets. The expression levels were standardized by comparing the Ct values of target to that of β -actin mRNA.

Intraperitoneal xenograft development assay

Intraperitoneal xenograft development was assessed as previously described (21, 49). Briefly, cells in the log phase were trypsinized and resuspended in PBS. Six-week-old athymic female nude mice (Hsd: athymic Nude-Foxn1nu, Harlan Sprague Dawley, Indianapolis, IN) were intraperitoneally injected with 1×10^7 cells per mouse. To determine metastatic potential of ovarian cancer cells, mice were sacrificed and autopsied three weeks after injection. Visible metastatic implants were collected and weighed. To determine the effect of AZD6244 and AZD0530 on metastatic colonization, mice were first injected with luciferase-expressing OVCAR3/Rac1G12V or SKOV3 cells for 12 days. AZD6244 and AZD0530 dissolved in 0.5% hydroxypropyl methylcellulose/0.1% Tween-80 were either alone or in combination administered orally to mice with aid of gavages daily. Doses for AZD6244 and AZD0530 were 50 mg/kg and 25 mg/kg respectively. The controls were mice given with vehicle daily. Tumor progression was monitored by examining fluorescence in Xenogen IVIS-200 *In Vivo* Imaging System on weekly base as previously described (50). Visible implants in peritoneal cavities were harvested and fixed for IHC. All procedures were approved by the Institution Animal Care Committee at Georgia Regents University.

Immunohistochemistry

Tumor tissues were collected immediately when tumor-bearing mice succumbed to death. Paraffin-embedded tissues were sectioned and subjected to IHC to detect vimentin and E-cadherin using the respective antibodies as previously described (21, 50).

Statistical analysis

Statistical analyses of *in vitro* invasion, cell shape change, cell migration, metastatic implant weights and gene expression levels were performed by ANOVA and student *t* test. Log rank test was used to analyze the significance in mouse survival. Statistical analyses were aided by SPSS (release 15.0; SPSS Inc). $P < 0.05$ was considered to be significant.

Supplementary Material

Refer to Web version on PubMed Central for supplementary material.

Acknowledgments

This work was supported by E-Institutes of Shanghai Municipal Education Commission (Project E03008), “085” First-Class Discipline Construction Innovation Science and Technology Support Project of Shanghai University of TCM (085ZY1206), NIH CA 187152 and DoD OC120313 (W81XWH-13-1-0122).

Grant Support: E-Institutes of Shanghai Municipal Education Commission (Project E03008), “085” First-Class Discipline Construction Innovation Science and Technology Support Project of Shanghai University of TCM (085ZY1206), NIH CA187152 and DoD OC120313 (W81XWH-13-1-0122).

References

- Jayson GC, Kohn EC, Kitchener HC, Ledermann JA. Ovarian cancer. *Lancet*. 2014; 384(9951): 1376–88. [PubMed: 24767708]
- Seward SM, Winer I. Primary debulking surgery and neoadjuvant chemotherapy in the treatment of advanced epithelial ovarian carcinoma. *Cancer metastasis reviews*. 2015; 34(1):5–10. [PubMed: 25597035]
- Thiery JP, Sleeman JP. Complex networks orchestrate epithelial-mesenchymal transitions. *Nat Rev Mol Cell Biol*. 2006; 7(2):131–42. [PubMed: 16493418]
- Thiery JP. Epithelial-mesenchymal transitions in tumour progression. *Nat Rev Cancer*. 2002; 2(6): 442–54. [PubMed: 12189386]
- Thiery JP, Acloque H, Huang RY, Nieto MA. Epithelial-mesenchymal transitions in development and disease. *Cell*. 2009; 139(5):871–90. [PubMed: 19945376]
- Lester RD, Jo M, Montel V, Takimoto S, Gonias SL. uPAR induces epithelial-mesenchymal transition in hypoxic breast cancer cells. *J Cell Biol*. 2007; 178(3):425–36. [PubMed: 17664334]
- Yang MH, Wu MZ, Chiou SH, Chen PM, Chang SY, Liu CJ, et al. Direct regulation of TWIST by HIF-1 α promotes metastasis. *Nature cell biology*. 2008; 10(3):295–305. [PubMed: 18297062]
- Wu Y, Deng J, Rychahou PG, Qiu S, Evers BM, Zhou BP. Stabilization of snail by NF- κ B is required for inflammation-induced cell migration and invasion. *Cancer cell*. 2009; 15(5):416–28. [PubMed: 19411070]
- Lopez-Novoa JM, Nieto MA. Inflammation and EMT: an alliance towards organ fibrosis and cancer progression. *EMBO Mol Med*. 2009; 1(6–7):303–14. [PubMed: 20049734]
- Prasanphanich AF, Arencibia CA, Kemp ML. Redox processes inform multivariate transdifferentiation trajectories associated with TGF β -induced epithelial-mesenchymal transition. *Free Radic Biol Med*. 2014; 76:1–13. [PubMed: 25088330]
- Davidson B, Trope CG, Reich R. Epithelial-mesenchymal transition in ovarian carcinoma. *Front Oncol*. 2012; 2:33. [PubMed: 22655269]
- Huang RY, Chung VY, Thiery JP. Targeting pathways contributing to epithelial-mesenchymal transition (EMT) in epithelial ovarian cancer. *Curr Drug Targets*. 2012; 13(13):1649–53. [PubMed: 23061545]
- Takai M, Terai Y, Kawaguchi H, Ashihara K, Fujiwara S, Tanaka T, et al. The EMT (epithelial-mesenchymal-transition)-related protein expression indicates the metastatic status and prognosis in patients with ovarian cancer. *J Ovarian Res*. 2014; 7:76. [PubMed: 25296567]
- Davidson B, Holth A, Hellesylt E, Tan TZ, Huang RY, Trope C, et al. The clinical role of epithelial-mesenchymal transition and stem cell markers in advanced-stage ovarian serous carcinoma effusions. *Human pathology*. 2015; 46(1):1–8. [PubMed: 25455994]
- Integrated genomic analyses of ovarian carcinoma. *Nature*. 2011; 474(7353):609–15. [PubMed: 21720365]
- Yoshida S, Furukawa N, Haruta S, Tanase Y, Kanayama S, Noguchi T, et al. Expression profiles of genes involved in poor prognosis of epithelial ovarian carcinoma: a review. *International journal of*

gynecological cancer : official journal of the International Gynecological Cancer Society. 2009; 19(6):992–7. [PubMed: 19820358]

17. Tan TZ, Miow QH, Miki Y, Noda T, Mori S, Huang RY, et al. Epithelial-mesenchymal transition spectrum quantification and its efficacy in deciphering survival and drug responses of cancer patients. *EMBO Mol Med*. 2014; 6(10):1279–93. [PubMed: 25214461]
18. Ponnusamy MP, Lakshmanan I, Jain M, Das S, Chakraborty S, Dey P, et al. MUC4 mucin-induced epithelial to mesenchymal transition: a novel mechanism for metastasis of human ovarian cancer cells. *Oncogene*. 2010; 29(42):5741–54. [PubMed: 20697346]
19. Chen D, Zhang Y, Wang J, Chen J, Yang C, Cai K, et al. MicroRNA-200c overexpression inhibits tumorigenicity and metastasis of CD117+CD44+ ovarian cancer stem cells by regulating epithelial-mesenchymal transition. *J Ovarian Res*. 2013; 6(1):50. [PubMed: 23842108]
20. Ahmed N, Abubaker K, Findlay J, Quinn M. Epithelial mesenchymal transition and cancer stem cell-like phenotypes facilitate chemoresistance in recurrent ovarian cancer. *Current cancer drug targets*. 2010; 10(3):268–78. [PubMed: 20370691]
21. Chen H, Wu X, Pan ZK, Huang S. Integrity of SOS1/EPS8/ABI1 tri-complex determines ovarian cancer metastasis. *Cancer Res*. 2010; 70(23):9979–90. [PubMed: 21118970]
22. Yamada SD, Hickson JA, Hrobowski Y, Vander Griend DJ, Benson D, Montag A, et al. Mitogen-activated protein kinase kinase 4 (MKK4) acts as a metastasis suppressor gene in human ovarian carcinoma. *Cancer Res*. 2002; 62(22):6717–23. [PubMed: 12438272]
23. Scita G, Nordstrom J, Carbone R, Tenca P, Giardina G, Gutkind S, et al. EPS8 and E3B1 transduce signals from Ras to Rac. *Nature*. 1999; 401(6750):290–3. [PubMed: 10499589]
24. Moustakas A, Heldin CH. Induction of epithelial-mesenchymal transition by transforming growth factor beta. *Semin Cancer Biol*. 2012; 22(5–6):446–54. [PubMed: 22548724]
25. Parvani JG, Taylor MA, Schiemann WP. Noncanonical TGF-beta signaling during mammary tumorigenesis. *J Mammary Gland Biol Neoplasia*. 2011; 16(2):127–46. [PubMed: 21448580]
26. Brabletz S, Bajdak K, Meidhof S, Burk U, Niedermann G, Firat E, et al. The ZEB1/miR-200 feedback loop controls Notch signalling in cancer cells. *The EMBO journal*. 2011; 30(4):770–82. [PubMed: 21224848]
27. Wu Y, Ginther C, Kim J, Mosher N, Chung S, Slamon D, et al. Expression of Wnt3 activates Wnt/beta-catenin pathway and promotes EMT-like phenotype in trastuzumab-resistant HER2-overexpressing breast cancer cells. *Molecular cancer research : MCR*. 2012; 10(12):1597–606. [PubMed: 23071104]
28. Lu Z, Ghosh S, Wang Z, Hunter T. Downregulation of caveolin-1 function by EGF leads to the loss of E-cadherin, increased transcriptional activity of beta-catenin, and enhanced tumor cell invasion. *Cancer cell*. 2003; 4(6):499–515. [PubMed: 14706341]
29. Radisky DC, Bissell MJ. NF-kappaB links oestrogen receptor signalling and EMT. *Nature cell biology*. 2007; 9(4):361–3. [PubMed: 17401385]
30. Cichon MA, Radisky DC. ROS-induced epithelial-mesenchymal transition in mammary epithelial cells is mediated by NF-kB-dependent activation of Snail. *Oncotarget*. 2014; 5(9):2827–38. [PubMed: 24811539]
31. Tian L, Li L, Xing W, Li R, Pei C, Dong X, et al. IRGM1 enhances B16 melanoma cell metastasis through PI3K-Rac1 mediated epithelial mesenchymal transition. *Scientific reports*. 2015; 5:12357. [PubMed: 26202910]
32. Zhang Z, Yang M, Chen R, Su W, Li P, Chen S, et al. IBP regulates epithelial-to-mesenchymal transition and the motility of breast cancer cells via Rac1, RhoA and Cdc42 signaling pathways. *Oncogene*. 2014; 33(26):3374–82. [PubMed: 23975422]
33. Yang WH, Lan HY, Huang CH, Tai SK, Tzeng CH, Kao SY, et al. RAC1 activation mediates Twist1-induced cancer cell migration. *Nature cell biology*. 2012; 14(4):366–74. [PubMed: 22407364]
34. Leng R, Liao G, Wang H, Kuang J, Tang L. Rac1 expression in epithelial ovarian cancer: effect on cell EMT and clinical outcome. *Medical oncology*. 2015; 32(2):329. [PubMed: 25585684]
35. Theriault BL, Shepherd TG, Mujoomdar ML, Nachtigal MW. BMP4 induces EMT and Rho GTPase activation in human ovarian cancer cells. *Carcinogenesis*. 2007; 28(6):1153–62. [PubMed: 17272306]

36. McGrail DJ, Kieu QM, Dawson MR. The malignancy of metastatic ovarian cancer cells is increased on soft matrices through a mechanosensitive Rho-ROCK pathway. *J Cell Sci.* 2014; 127(Pt 12):2621–6. [PubMed: 24741068]
37. Gou WF, Zhao Y, Lu H, Yang XF, Xiu YL, Zhao S, et al. The role of RhoC in epithelial-to-mesenchymal transition of ovarian carcinoma cells. *BMC cancer.* 2014; 14:477. [PubMed: 24986540]
38. Huang RY, Wong MK, Tan TZ, Kuay KT, Ng AH, Chung VY, et al. An EMT spectrum defines an anoikis-resistant and spheroidogenic intermediate mesenchymal state that is sensitive to e-cadherin restoration by a src-kinase inhibitor, saracatinib (AZD0530). *Cell Death Dis.* 2013; 4:e915. [PubMed: 24201814]
39. Condello S, Cao L, Matei D. Tissue transglutaminase regulates beta-catenin signaling through a c-Src-dependent mechanism. *FASEB J.* 2013; 27(8):3100–12. [PubMed: 23640056]
40. Cheng S, Guo J, Yang Q, Yang X. Crk-like adapter protein regulates CCL19/CCR7-mediated epithelial-to-mesenchymal transition via ERK signaling pathway in epithelial ovarian carcinomas. *Medical oncology.* 2015; 32(3):47. [PubMed: 25636509]
41. Javle MM, Gibbs JF, Iwata KK, Pak Y, Rutledge P, Yu J, et al. Epithelial-mesenchymal transition (EMT) and activated extracellular signal-regulated kinase (p-Erk) in surgically resected pancreatic cancer. *Annals of surgical oncology.* 2007; 14(12):3527–33. [PubMed: 17879119]
42. Mandal M, Myers JN, Lippman SM, Johnson FM, Williams MD, Rayala S, et al. Epithelial to mesenchymal transition in head and neck squamous carcinoma: association of Src activation with E-cadherin down-regulation, vimentin expression, and aggressive tumor features. *Cancer.* 2008; 112(9):2088–100. [PubMed: 18327819]
43. Bid HK, Roberts RD, Manchanda PK, Houghton PJ. RAC1: an emerging therapeutic option for targeting cancer angiogenesis and metastasis. *Molecular cancer therapeutics.* 2013; 12(10):1925–34. [PubMed: 24072884]
44. Chen H, Zhu G, Li Y, Padia RN, Dong Z, Pan ZK, et al. Extracellular signal-regulated kinase signaling pathway regulates breast cancer cell migration by maintaining slug expression. *Cancer Res.* 2009; 69(24):9228–35. [PubMed: 19920183]
45. Hong S, Noh H, Teng Y, Shao J, Rehmani H, Ding HF, et al. SHOX2 Is a Direct miR-375 Target and a Novel Epithelial-to-Mesenchymal Transition Inducer in Breast Cancer Cells. *Neoplasia.* 2014; 16(4):279–90. e5. [PubMed: 24746361]
46. Li Y, Zhang M, Chen H, Dong Z, Ganapathy V, Thangaraju M, et al. Ratio of miR-196s to HOXC8 messenger RNA correlates with breast cancer cell migration and metastasis. *Cancer Res.* 2010; 70(20):7894–904. [PubMed: 20736365]
47. Li Y, Guo Z, Chen H, Dong Z, Ding H, Huang S. HOXC8-Dependent Cadherin 11 Expression Facilitates Breast Cancer Cell Migration through Trio and Rac. *Genes & Cancer.* 2012
48. Li Y, Chao F, Huang B, Liu D, Kim J, Huang S. HOXC8 promotes breast tumorigenesis by transcriptionally facilitating cadherin-11 expression. *Oncotarget.* 2014; 5(9):2596–607. [PubMed: 24810778]
49. Yang L, Fang D, Chen H, Lu Y, Dong Z, Ding HF, et al. Cyclin-dependent kinase 2 is an ideal target for ovary tumors with elevated cyclin E1 expression. *Oncotarget.* 2015; 6(25):20801–12. [PubMed: 26204491]
50. Hu Q, Lu YY, Noh H, Hong S, Dong Z, Ding HF, et al. Interleukin enhancer-binding factor 3 promotes breast tumor progression by regulating sustained urokinase-type plasminogen activator expression. *Oncogene.* 2013; 32(34):3933–43. [PubMed: 22986534]

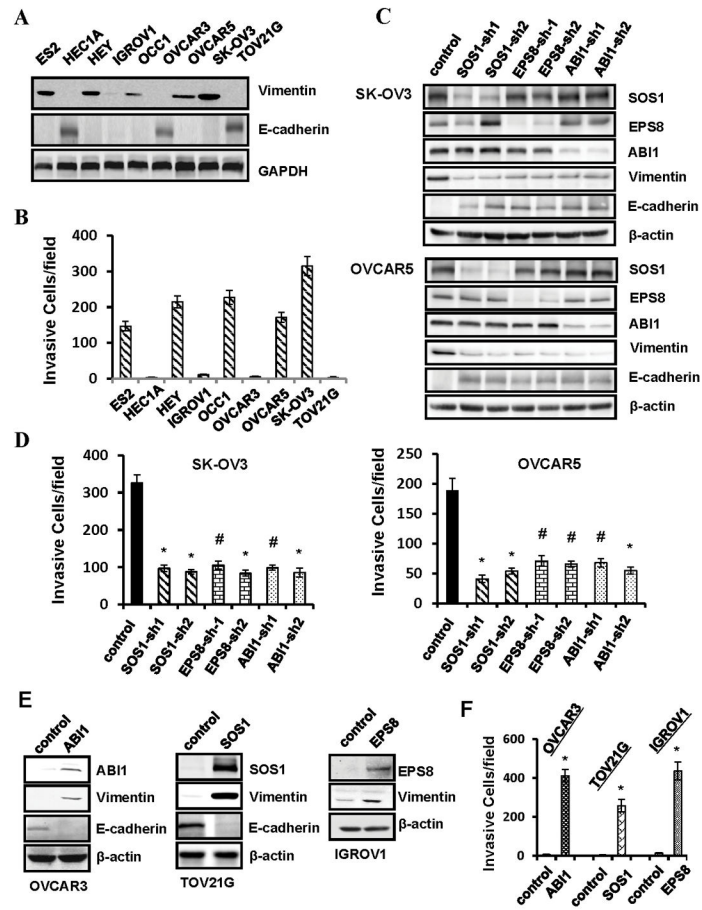


Figure 1. Presence of SOS1/EPS8/ABI1 complex is correlated with EMT in ovarian cancer cells. **A.** Western blot analysis of E-cadherin, vimentin and GAPDH in various ovarian cancer cell lines. **B.** Matrigel *in vitro* invasion assay was performed to analyze the invasiveness of various ovarian cancer cell lines. Data are means \pm SE (n = 4). **C.** SK-OV3 and OVCAR5 cells were transduced with lentiviral vectors containing scramble sequence, SOS1, EPS8, or ABI1 shRNA for 4 days followed by Western blotting to detect SOS1, EPS8, ABI1, E-cadherin, vimentin and β -actin with the respective antibodies. **D.** SK-OV3 and OVCAR5 cells were lentivirally transduced with lentiviral vectors containing scramble sequence, SOS1, EPS8, or ABI1 shRNA for 4 days followed by the analysis of *in vitro* invasiveness using Matrigel invasion chambers. Data are means \pm SE (n = 4). *, $p < 0.005$; #, $p < 0.05$ vs control. **E.** OVCAR3, TOV21G and IGROV1 cells were transduced with lentiviral vector containing ABI1, SOS1 or EPS8 expression cassette respectively for 4 days. Cells were then lysed and lysates subjected to Western blotting to detect SOS1, EPS8, ABI1, E-cadherin, vimentin and β -actin with the respective antibodies. **F.** Matrigel invasion assay to analyze the *in vitro* invasiveness of OVCAR3/ABI1, TOV21G/SOS1 and IGROV1/EPS8 cells. Data are means \pm SE (n = 4). *, $p < 0.005$ vs control.

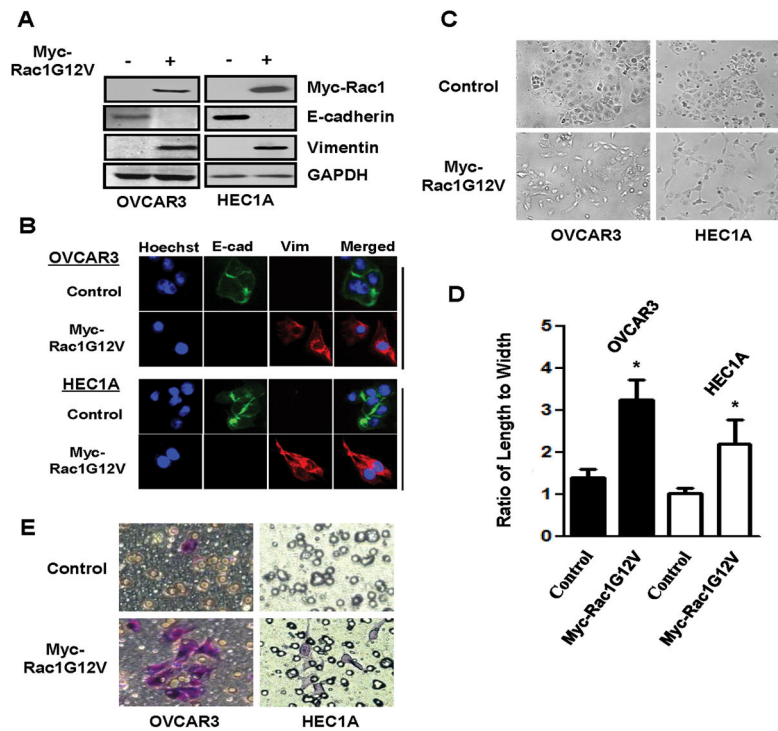


Figure 2. Constitutively active Rac1 induces EMT in ovarian cancer cells

A. OVCAR3 and HEC-1A cells were lentivirally transduced with empty vector (control) or vector containing Myc-tagged Rac1G12V for 4 days. Cells were lysed and cell lysates were subjected to Western blotting to detect Myc-tagged Rac1G12V, E-cadherin, vimentin and GAPDH with the respective antibodies. **B.** Immunofluorescence staining was performed to detect E-cadherin and vimentin on control and Rac1G12V-transduced OVCAR3 and HEC-1A cells. **C.** Morphologies of control and Rac1G12V-transduced OVCAR3 and HEC-1A cells. **D.** Ratio of length to width in control and Rac1G12V-transduced OVCAR3 and HEC1A cells. Data are means \pm SE (n = 104). *, $p < 0.005$ vs control. **E.** Overnight-cultured control and Rac1G12V-transduced OVCAR3 and HEC-1A cells were detached with PBS containing 10mM EDTA, then washed and plated into upper chambers of Matrigel invasion assay system for 24 h. Cells on the undersurface of upper chambers were stained with crystal solution and visualized under a phase-contrast microscope.

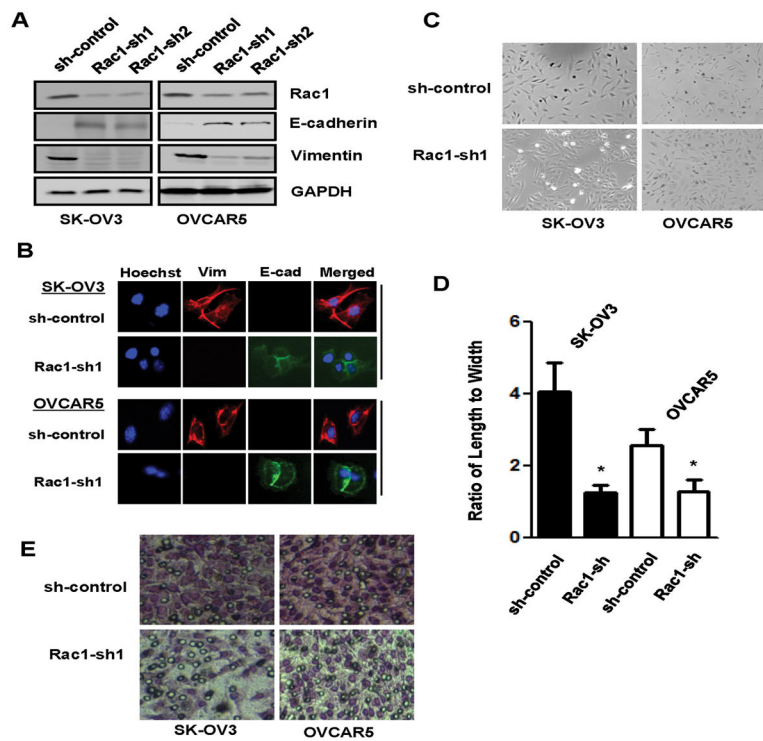


Figure 3. Knockdown of Rac1 leads to the suppression of EMT in ovarian cancer cells
A. SK-OV3 and OVCAR5 cells were transduced with lentiviral vectors containing scramble sequence or Rac1 shRNA for 4 days followed by Western blotting to detect Rac1, E-cadherin, vimentin and GAPDH with the respective antibodies. **B.** Immunofluorescence staining of E-cadherin and vimentin of control and Rac1-knockdown SK-OV3 and OVCAR5 cells. **C.** Morphologies of control and Rac1-knockdown SK-OV3 and OVCAR5 cells. **D.** Ratio of length to width in control and Rac1-knockdown SK-OV3 and OVCAR5 cells. Data are means \pm SE (n = 111). *, $p < 0.005$ vs control. **E.** *In vitro* invasion of control and Rac1-knockdown SK-OV3 and OVCAR5 cells.

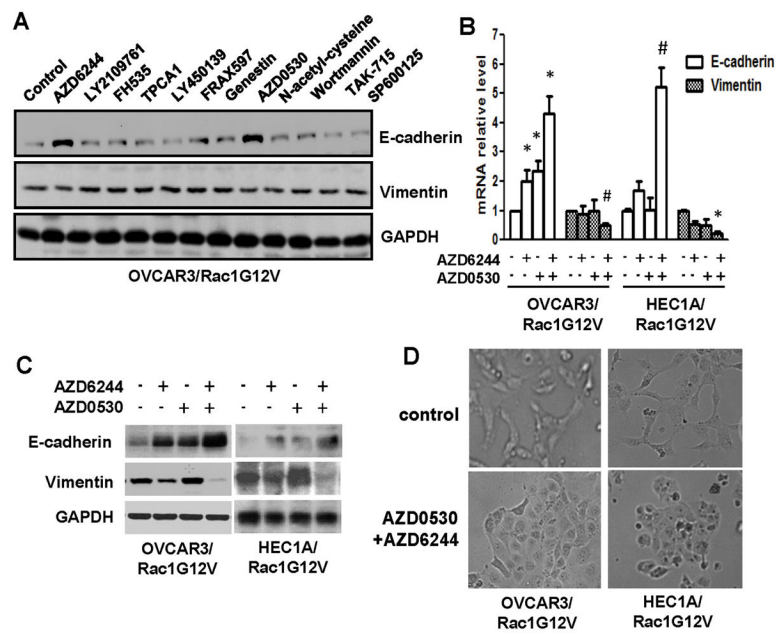


Figure 4. Rac1-led EMT depends on the activities of MEK1/2 and Src

A. OVCAR3/Rac1G12V cells were treated with various inhibitors for 3 days, then lysed and cell lysates were subjected to Western blotting to detect E-cadherin, vimentin and GAPDH with the respective antibodies. **B.** OVCAR3/Rac1G12V and HEC1A/Rac1G12V cells were treated with 0.5 μ M AZD0530 or 5 μ M AZD6244 alone or together for 3 days, total RNA was then extracted and qRT-PCR was performed to determine the levels of E-cadherin, vimentin and β -actin mRNA. Data are means \pm SE (n = 3). *, $p < 0.005$ vs vehicle control; #, $p < 0.01$ vs vehicle control. **C.** OVCAR3/Rac1G12V and HEC1A/Rac1G12V cells were treated with 0.5 μ M AZD0530 or 5 μ M AZD6244 alone or together for 3 days, then lysed and cell lysates were subjected to Western blotting to detect E-cadherin, vimentin and GAPDH with the respective antibodies. **D.** Morphologies of OVCAR3/Rac1G12V and HEC1A/Rac1G12V cells treated with vehicle or combination of AZD0530 and AZD6244 for 3 days.

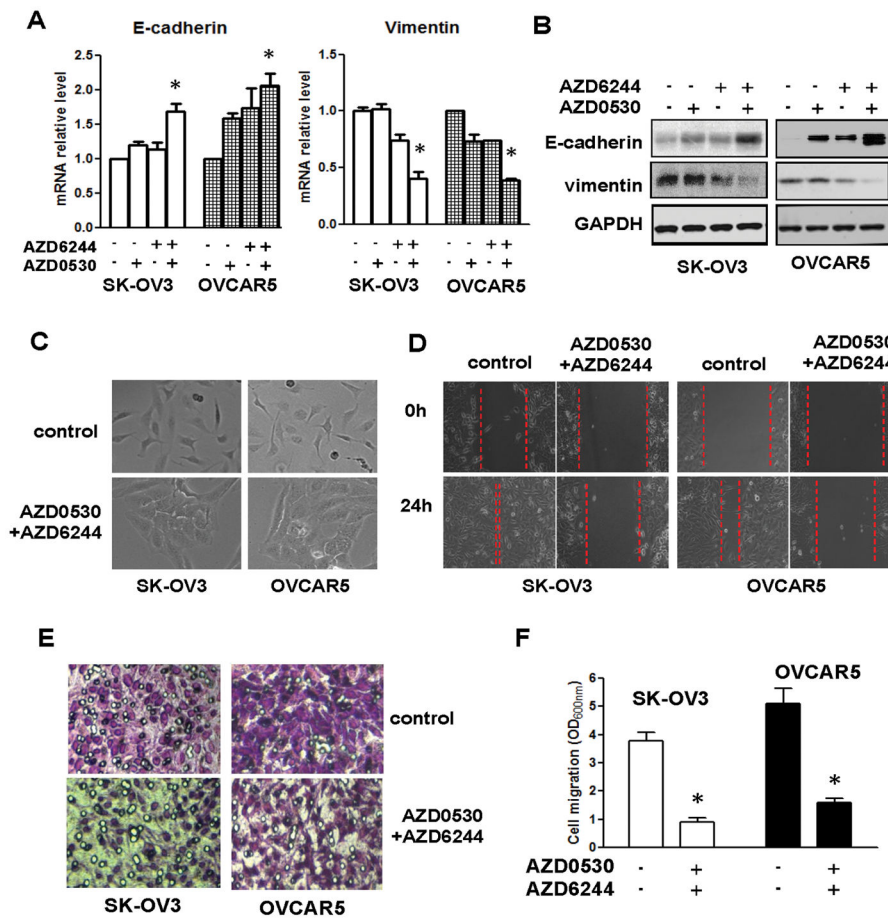


Figure 5. Sustained EMT in ovarian cancers necessitates the activity of MEK1/2 and Src
A. SK-OV3 and OVCAR5 cells were treated with 0.5 μ M AZD0530 or 5 μ M AZD6244 alone or together for 3 days, total RNA was then isolated and qRT-PCR was performed to determine the levels of E-cadherin, vimentin and β -actin mRNA. Data are means \pm SE (n = 3). *, $p < 0.01$ vs vehicle control. **B.** SK-OV3 and OVCAR5 cells were treated with 0.5 μ M AZD0530 or 5 μ M AZD6244 alone or together for 3 days, then lysed and cell lysates were subjected to Western blotting to detect E-cadherin, vimentin and GAPDH with the respective antibodies. **C.** Morphologies of SK-OV3 and OVCAR5 cells treated with vehicle or combination of AZD0530 and AZD6244 for 3 days. **D.** SK-OV3 and OVCAR5 were grown to confluent monolayer cells in the presence or absence of AZD0530/AZD6244 for 3 days. A scratch was made with a fine pipette tip and dislodged cells were washed away with serum-free medium. The cells were fed with medium containing 1% FCS with or without AZD0530/AZD6244 and images were taken at 0 and 24 h under a phase contrast microscope. **E.** SK-OV3 and OVCAR5 cells were treated with vehicle or combination of AZD0530 and AZD6244 for 3 days followed by the analysis of cell migration using Transwells. Cells remained on the undersurface of Transwells were stained with crystal violet and visualized under a phase-contrast microscope. **F.** Stained cells on undersurface of Transwells were solubilized and read at wavelength of 600nm on a microplate reader. Data are means \pm SE (n = 4). *, $p < 0.005$ vs control.

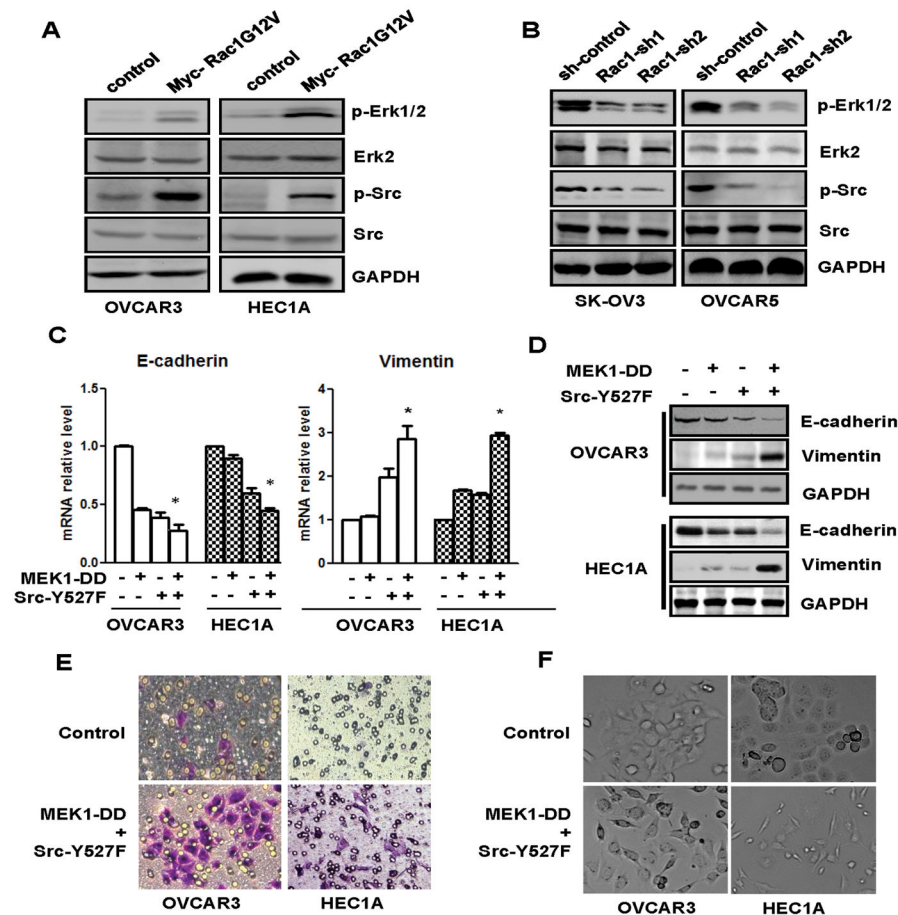


Figure 6. Simultaneous activation of MEK1/2 and Src pathways leads to EMT in ovarian cancer cells

A. OVCAR3/Rac1G12V and HEC1A/Rac1G12V cells were lysed and cell lysates were subjected to Western blotting to detect p-Erk1/2, Erk2, p-Src, Src and GAPDH using the respective antibodies. **B.** Control and Rac1-knockdown SK-OV3 and OVCAR5 cells lysed and cell lysates were subjected to western blotting to detect p-Erk1/2, Erk2, p-Src, Src and GAPDH using the respective antibodies. **C.** OVCAR3 and HEC1A cells were transduced with lentiviral vector encoding MEK1-DD or Src-Y527F individually or together for 4 days. Total RNA was extracted from these cells and then subjected to qRT-PCR to analyze the levels of E-cadherin, vimentin and β -actin mRNA. Data are means \pm SE (n = 4). *, $p < 0.01$ vs control. **D.** OVCAR3 and HEC1A cells transduced with lentiviral vector encoding MEK1-DD or Src-Y527F individually or together were lysed and cell lysates were subjected to Western blotting to detect E-cadherin, vimentin and GAPDH with the respective antibodies. **E.** OVCAR3 and HEC1A cells transduced with empty vector or together with vectors containing MEK1-DD and Src-Y527F were analyzed for their *in vitro* invasiveness using Matrigel invasion chambers. Cells remained on the undersurface of invasion chambers were stained and visualized under a phase-contrast microscope. **F.** Morphologies of OVCAR3/Rac1G12V and HEC1A/Rac1G12V cells treated with vehicle or combination of AZD0530 and AZD6244 for 3 days.

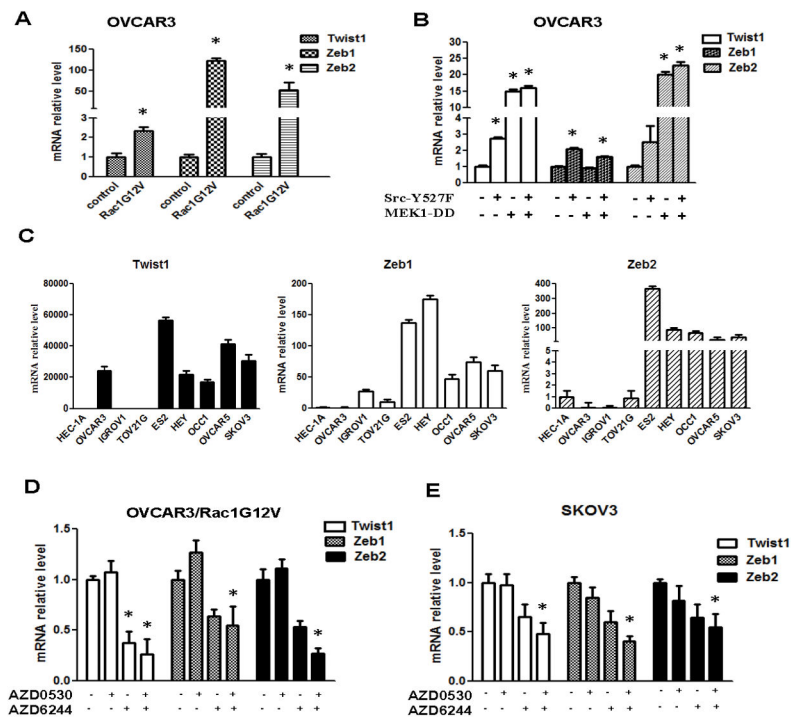


Figure 7. Rac1-MEK/Src signaling axis promotes the expression of Twist1 and Zeb1/2 in ovarian cancer cells

A. qRT-PCR analysis of Twist, Zeb1 and Zeb2 in OVCAR3/Rac1G12V cells. Data are means \pm SE (n = 3). *, $p < 0.05$ vs control. **B.** qRT-PCR analysis of Twist, Zeb1 and Zeb2 in OVCAR3 cells transduced with MEK1-DD and Src-Y527F individually or together. Data are means \pm SD (n = 3). *, $p < 0.05$ vs control. **C.** qRT-PCR analysis of Twist, Zeb1 and Zeb2 in various ovarian cancers. Data are means \pm SD (n = 3). **D.** OVCAR3/Rac1G12V cells were treated with 0.5 μ M AZD0530 or 5 μ M AZD6244 alone or together for 3 days. Cells were extracted for total RNA and total RNA was subjected to qRT-PCR to measure the levels of Twist, Zeb1 and Zeb2 mRNA. Data are means \pm SD (n = 3). *, $p < 0.05$ vs vehicle. **E.** SKOV3 cells were treated with 0.5 μ M AZD0530 or 5 μ M AZD6244 alone or together for 3 days. Cells were extracted for total RNA and total RNA was subjected to qRT-PCR to measure the levels of Twist, Zeb1 and Zeb2 mRNA. Data are means \pm SD (n = 3). *, $p < 0.05$ vs vehicle.

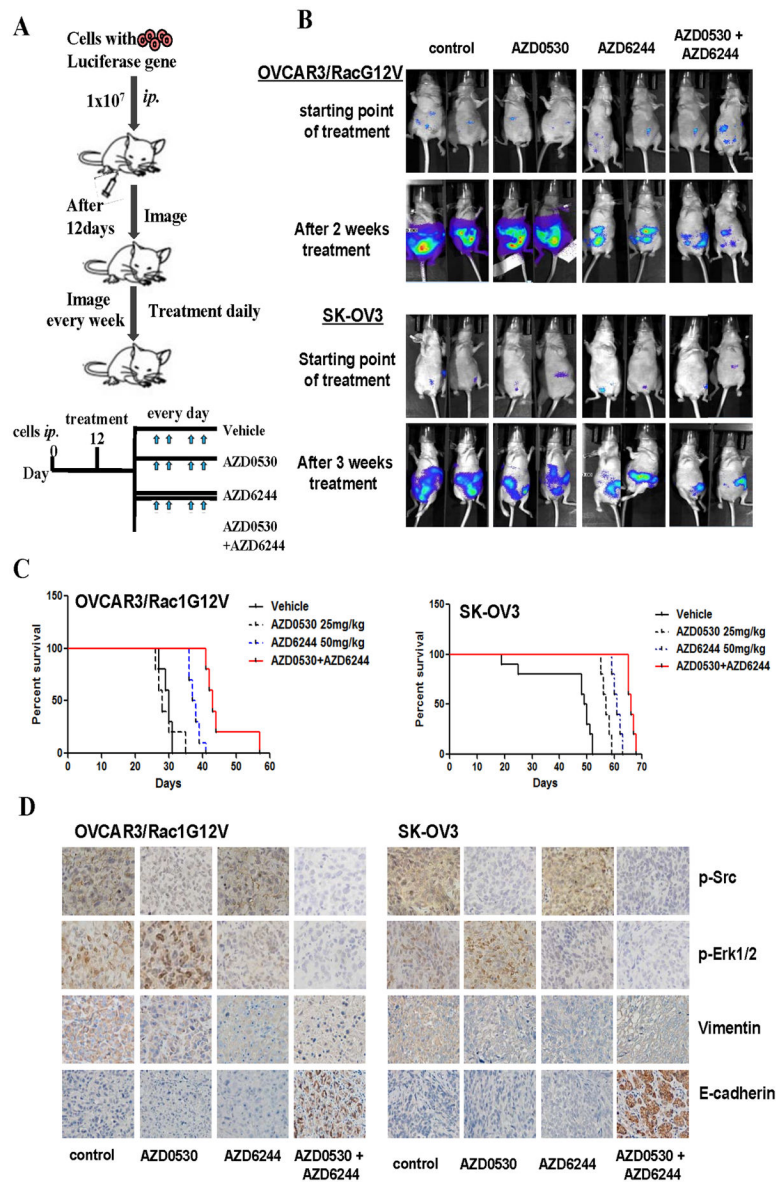


Figure 8. Combined use of MEK1/2 AND Src inhibitors suppresses ovarian cancer progression
A. Flow chart of therapy scheme. **B.** OVCAR3/Rac1V12G or SK-OV3 cells (1×10^7 cells/mouse) were injected *i.p.* to nude mice for 12 days followed by administration of 50mg/kg AZD6244 or 25mg/kg AZD0530 individually or together. Tumors were imaged in Xenogen system. **C.** Kaplan-Meier analysis of animal endpoint survival following treatment with AZD6244 or AZD0530 individually or in combination. **D.** Representative pictures of immunohistochemical staining of phosphor-Src, phosphor-Erk, E-cadherin and Vimentin in tumor tissues. Scale bars, 50 μ m.